

PAPER • OPEN ACCESS

Conversion of carbon dioxide and methane to syngas over Ni/SiO₂ catalyst prepared from waste palm oil fuel ash

To cite this article: H A Razak *et al* 2019 *IOP Conf. Ser.: Earth Environ. Sci.* **220** 012058

View the [article online](#) for updates and enhancements.

Conversion of carbon dioxide and methane to syngas over Ni/SiO₂ catalyst prepared from waste palm oil fuel ash

H A Razak¹, N Abdullah¹, J Gasang¹, H D Setiabudi^{1,2}, C S Yee^{1,2} and N Ainirazali¹

¹Faculty of Chemical and Natural Resources Engineering, Universiti Malaysia Pahang, 26300 Gambang, Kuantan, Pahang, Malaysia

²Centre of Excellence for Advance Research in Fluid Flow, Universiti Malaysia Pahang, 26300 Gambang, Kuantan, Pahang, Malaysia

Abstract. Carbon dioxide (CO₂) reforming of methane (CH₄) over nickel (Ni)-supported SiO₂ catalyst is a greener approach as this pathway transforms greenhouse gases into gas energy. SiO₂ support was synthesized from waste palm oil fuel ash (POFA) with different Ni loading (Ni/SiO₂). The SiO₂(POFA) was synthesized by drying the treated POFA overnight and calcined at 600 °C for 6 h. The Ni/SiO₂ (POFA) catalyst with different Ni loading were synthesized by impregnation method. The physicochemical properties of the Ni/SiO₂ (POFA) were characterized using nitrogen adsorption-desorption, x-ray diffraction (XRD), and fourier transform infrared (FTIR) spectroscopy. The catalytic performance of the Ni/SiO₂ (POFA) was carried out at 800 °C and atmospheric pressure with CO₂/CH₄ feed ratio of 1/1. The SiO₂ (POFA) possess a good support material as it has a high surface area 6.95 m² g⁻¹ and assist well dispersion of Ni as evidenced by BET analysis. Higher catalytic activity was achieved at 53.10% of CO₂ conversion and 67.6% of CH₄ conversion over 5Ni/SiO₂ (POFA). However, lower CO₂ conversion of Ni/SiO₂ (POFA) catalyst was due to the larger particle size of Ni and weak metal-support interaction in Ni/SiO₂ (POFA). This finding proved that the waste POFA can replace the commercial SiO₂ for catalytic gas reaction and solve the environmental problem.

1. Introduction

The past few years, the carbon dioxide reforming of methane (DRM) has been investigated for carbon dioxide utilization and syngas generation ($\text{CH}_4 + \text{CO}_2 \rightarrow 2\text{CO} + 2\text{H}_2$). However, the main challenges for the widespread application of DRM resides in catalyst performance is the quick deactivation of catalysts, as a result of carbon deposition [1]. Previous researchers reported that the supported noble metal catalysts such as platinum (Pt), palladium (Pd), and rhodium (Rh) are active and stable [2]. However, due to the high cost of noble metal, most researchers have been focusing on metal-based catalysts, particularly nickel. Ni was reported to have high activity and selectivity and are less expensive than noble metal [3]. Catalyst plays an important role in order to determine the performance of Ni-based catalyst and also to prevent coke formation. Thus, SiO₂ support was chosen due to good thermostability, availability, and relatively high specific area [4]. It has been reported that silica oxide (SiO₂) is successfully used as a catalyst support in fluidized bed reactor due to its high mechanical strength [5]. The high cost of commercial SiO₂ required for the large-scale manufacture has motivated the utilization of agricultural waste materials.

Several researchers have focused on the use of agricultural waste such as rice husk, corn cob ash, sugarcane bagasse, bamboo leaves, and palm oil fuel ash as a renewable source for production of silica



oxide (SiO_2) [6–10]. Malaysia is a major worldwide producer of palm oil which contributes around 47 %, thus the waste from this industry is growing rapidly and abundant which can give negative effect to human health and environment [6]. Palm oil fuel ash (POFA) is the major waste formed in this industry by the burning process of fibers, shells, empty fruit bunches (EFB) and few others [7]. It was reported that POFA is rich with SiO_2 content material with 48.99 % of SiO_2 followed by minor content of CaO (11.69 %), LOI (10.51 %), Fe_2O_3 (4.89 %), Al_2O_3 (3.78 %), MgO (1.22 %), and N_2O (0.73 %) [8]. Thus, in order to produce economical catalyst, palm oil fuel ash has been chosen as an alternative of the SiO_2 source. POFA was recently found to be a sustainable source of silica because it is composed with highly reactive SiO_2 . Therefore, POFA may be potentially be utilized as a sustainable source of SiO_2 .

In this study, the POFA waste was utilized to produce SiO_2 as the support material for Ni loading. The effect of different Ni content supported onto SiO_2 towards the catalyst properties and catalytic testing of CO_2 reforming of CH_4 were reported.

2. Materials and Method

2.1. Synthesis of SiO_2

The raw waste material, Palm Oil Fuel Ash (POFA) used in this study was obtained from FELDA Lepar Hilir Palm Oil Mill, Gambang, Pahang. The raw POFA was calcined in the furnace at the temperature of 600 °C for 6 h to remove unburnt and unspent biomass residue. POFA was treated with 2 M HCl solution using reflux method and constantly stirred at 100 °C for 3 h. The HCl-treated POFA were filtered and washed thoroughly with distilled water until pH 7 and named as APOFA. Then, the APOFA were dried for 12 h at 110 °C followed by calcination at 600 °C for 6 h.

2.2. Preparation of Ni/ SiO_2

The incipient wetness impregnation method was employed for producing Ni/ SiO_2 catalyst. The SiO_2 supports were added in the calculated amount of NiNO_3 solution respective to the Ni content. The mixture was then constantly stirred at 80 °C until all the water nearly evaporated. The resulting solid was dried at 110 °C for 12 h followed by calcination at 550 °C for 3 h. The prepared samples with different Ni-loaded were denoted as xNi/ SiO_2 , where x represents the loading amount (wt%).

2.3. Characterization

The chemical composition of raw POFA and treated POFA-HCl was analyzed by the X-ray Fluorescence (Model S8 Tiger). The crystalline structure of the catalysts was examined using X-ray powder diffraction (XRD) recorded on powder diffractometer (Philips X' Pert PD) with a step-scan mode at $2\theta=20-80^\circ$ with Cu and $\text{K}\alpha$ ray, operating at 30.0 kV and 15.0 mA as the X-ray source. For estimating the NiO crystal size, it was done by using the Scherrer equation (as shown in equation 1).

$$D_{\text{NiO}} = \frac{0.9\lambda}{B\cos\theta} \quad (1)$$

The BET surface area and structure properties of Ni/ SiO_2 catalyst were measured by using AUTOSORB-1 model ASI MP-LP analyser. The sample was degassed at 120 °C for 3 h under vacuum prior to measurement. The specific surface area was calculated from the adsorption curve based on the Brunauer-Emmet-Teller (BET) method. While, the pore volume was calculated according to the Barrett, Joyner, and Halenda (BJH) method.

The interaction between Ni and SiO_2 was determined by Fourier transform infrared (FTIR) spectra using a Thermo Nicolet Avatar 370 DTGS model. The samples were prepared by compressing in an evacuable die under 10-ton pressure for 5 min in order to yield transparent discs suitable for mounting in the spectrometer. The infrared spectrum was recorded in the region of 1200- 600 cm^{-1} . Thermal stability and structure destruction of the SiO_2 and Ni/ SiO_2 catalysts were determined by

Thermogravimetric analysis (TGA) (PL-TGA) at a heating rate $10\text{ }^{\circ}\text{C min}^{-1}$ up to $900\text{ }^{\circ}\text{C}$. 9 mg of samples were weighted with flowrate 40 mL min^{-1} in the presence of nitrogen as an inert purge.

2.4. Catalyst Testing

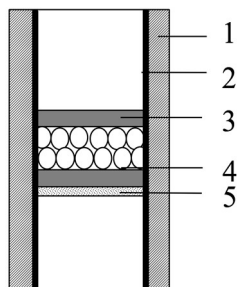


Figure 1. Vertical tube furnace diagram of (1) electric furnace, (2) tube stainless steel, (3) pallet catalyst, (4) quartz wool, (5) supporting pad.

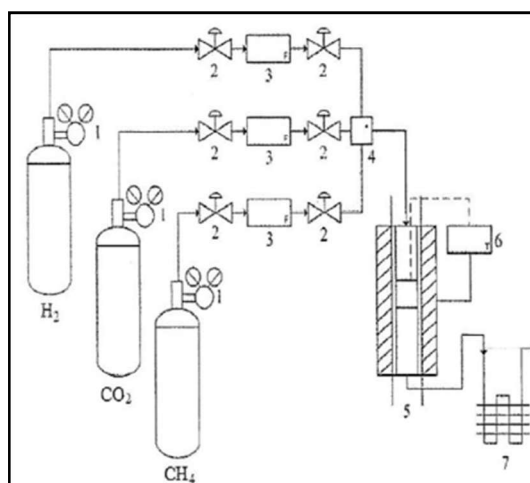


Figure 2. Schematic diagram of CO_2 reforming of CH_4 (1) regulator, (2) valve, (3) mass flow controller, (4) gas chamber, (5) vertical tube furnace, (6) temperature controller, (7) condenser.

The catalytic activity of the Ni/SiO_2 catalyst for CO_2 reforming of CH_4 was conducted in a stainless fixed bed reactor (i.d. 11 mm, length 417 mm) as shown in figure 1 under atmospheric pressure at $800\text{ }^{\circ}\text{C}$. Prior to the schematic diagram as shown in figure 2, 0.2 g of catalyst was reduced in 50 mL min^{-1} of hydrogen flow for 1 h at $700\text{ }^{\circ}\text{C}$. The reactant of $\text{CH}_4:\text{CO}_2:\text{N}_2$ with ratio 1:1:1 was fed into the reactor at $800\text{ }^{\circ}\text{C}$ within 5 h time-on-stream (TOS). The effluent gas was analyzed per hour by an Agilent gas chromatography (AGILENT 6890 N) equipped with a thermal conductivity detector (TCD). The conversion of CO_2 , CH_4 and H_2/CO ratio is defined as follows:

$$\text{CO}_2 \text{ conversion, } X_{\text{CO}_2} (\%) = \frac{F_{\text{CO}_2(\text{in})} - F_{\text{CO}_2(\text{out})}}{F_{\text{CO}_2(\text{in})}} \times 100\% \quad (2)$$

$$\text{CH}_4 \text{ conversion, } X_{\text{CH}_4} (\%) = \frac{F_{\text{CH}_4(\text{in})} - F_{\text{CH}_4(\text{out})}}{F_{\text{CH}_4(\text{in})}} \times 100\% \quad (3)$$

where F is the molar flow rate for the particular compound. The product distribution ratio, H_2/CO was calculated based on the equation:

$$\frac{H_2}{CO} = \frac{F_{H_2}}{F_{CO}} \quad (4)$$

3. Result and Discussion

3.1. POFA and APOFA Characterization

The chemical compound and composition of POFA and APOFA were presented in Table 1. It can be seen that the SiO_2 possessed the highest composition percentage in POFA and APOFA. However, the percentage of the SiO_2 was increased up to 85.46% after treatment of POFA with 2M HCl known as APOFA. The increment of the SiO_2 content was due to the acid treatment of POFA that helps to remove impurities of POFA by reducing other chemical composition [9]. Irfan Khan et al. [10] reported that silica content of palm ash after treated with HCl was increased up to 55 % due to the removal of metallic impurities in POFA. The XRF analysis proved that the waste APOFA rich with SiO_2 can be considered as a support material in replacing the commercial SiO_2 .

Table 1. Chemical composition of POFA and APOFA.

Chemical composition	SiO_2	Al_2O_3	Fe_2O_3	CaO	K_2O	P_2O_5	MgO	TiO_2	Others
POFA	47.71	7.73	8.95	13.36	10.02	5.27	2.46	0.97	3.53
APOFA	85.46	1.84	3.80	1.48	3.90	1.44	0.68	0.90	0.50

3.2. Characterization of Ni/SiO₂ catalyst

Figure 3 shows the XRD patterns of the parent SiO_2 and Ni/SiO₂ catalysts. XRD pattern for pure SiO_2 found major phases as cristobalite at peak 20.9°, 26.6°, 32.46°, 50.3°, 68.4° [11]. APOFA provides more SiO_2 peak that prove high purity of silica able to produce from waste POFA, in agreement with the XRD analysis. It was observed that all samples exhibited strong peaks at 2θ of 20.9° and 26.6°, which corresponding to the silica. However, the peak intensities of SiO_2 were reduces as the Ni loading was increased due to the partial collapse of SiO_2 . It has been reported that an increase of the Ni content caused slight decreased of the peaks designating structural degradation of the support [12]. While, the characteristic peaks assigned to the NiO were observed for all Ni/SiO₂ at 2θ of 43.2°, 59.9°, and 75.6° [13]. The increase in Ni loading led to the increase of the NiO peak intensity, indicating that more NiO were dispersed on the surface of the SiO_2 support. The Scherrer equation was used to estimate the NiO crystal size and the results were tabulated in Table 2. The average crystal sizes of 1Ni/SiO₂, 3Ni/SiO₂, 5Ni/SiO₂, and 10Ni/SiO₂ were 52.92, 64.80, 70.96, 93.68 nm respectively. The increment in NiO crystallite size with the increase in Ni loading was due to the agglomeration of more NiO particles on the support surfaces. According to Sidik et al. [14], the introduction of Ni notably increased the intensity of the diffraction peaks of Ni become sharper, which indicates that Ni crystals size increases with the Ni content from (1wt% to 10wt%) that form more crystalline phase of NiO on the SiO_2 .

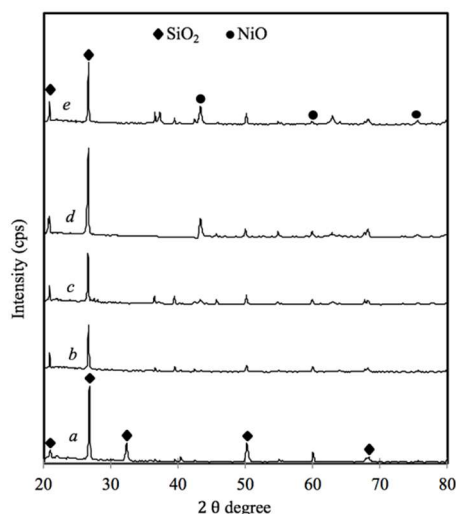


Figure 3. Wide angle XRD patterns of (a) SiO₂ (b) 1Ni/SiO₂ (c) 3Ni/SiO₂ (d) 5Ni/SiO₂ (e) 10Ni/SiO₂

The nitrogen adsorption–desorption of Ni/SiO₂ catalysts are presented in Figure 4. All the N₂ adsorption–desorption isotherms showed a similar trend of typical type IV with H4 hysteresis loops of Ni/SiO₂ [15]. Physical properties of the SiO₂ and Ni/SiO₂ catalysts at different Ni loading are summarized in Table 2. The introduction of Ni from 1 to 10 wt% caused the decreased of BET surface area from 6.34 m² g⁻¹ to 3.23 m² g⁻¹. The lowest BET surface area (3.23 m² g⁻¹) was obtained for the 10Ni/SiO₂ catalysts, due to more pores blockage occurred in the pores when 10wt% of Ni was loaded. Previous researchers reported that the effect of the amount of metal loading caused the difference of BET surface area for Ni/MSN catalysts, reported by Sidik et al. [14]. It found that the increase in the metal loading led to a decrease in the surface area as the catalyst pores were blocked by the metal species. It showed that the pore volume of Ni/SiO₂ catalyst was increased when the Ni loading increased up to 5 wt%, due to the agglomeration of Ni particles at the pore of particle SiO₂. However, the sudden decreased in the pore volume of 10Ni/SiO₂ to 0.0254 cm³ g⁻¹ was probably due to the deposition of Ni particles on the support and interparticles support [16].

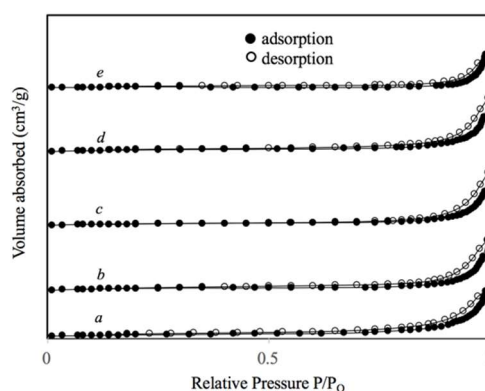
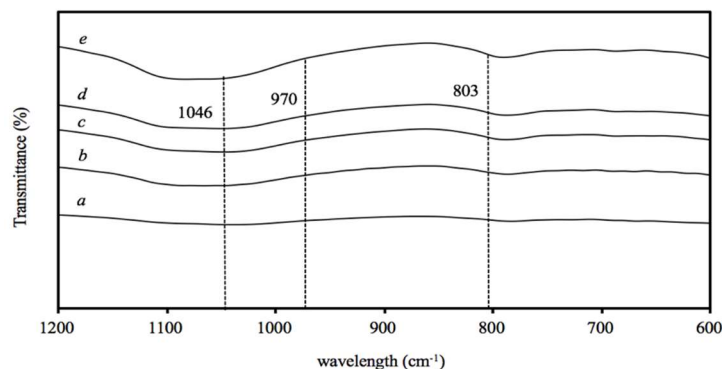


Figure 4. Nitrogen adsorption/desorption isotherms of (a) SiO₂ (b) 1Ni/SiO₂ (c) 3Ni/SiO₂ (d) 5Ni/SiO₂ and (e) 10Ni/SiO₂

Table 2. Physical of SiO₂, 1Ni/SiO₂, 3Ni/SiO₂, 5Ni/SiO₂, 10Ni/SiO₂

Catalyst Ni/SiO ₂	BET surface area (m ² g ⁻¹)	Pore volume (cm ³ g ⁻¹)	Ni particle size ^a (nm)
SiO ₂	6.95	0.0352	0
1	6.34	0.0389	52.9
3	6.22	0.0411	64.8
5	5.72	0.0416	70.9
10	3.23	0.0254	93.6

The FTIR spectra of SiO₂ and Ni/SiO₂ catalysts with different Ni loading in the range of 1200-600 cm⁻¹ were presented in Figure 5. The bands are attributed to the vibrations of the stretching and bending modes of Si-O units. The transmittance bands for all samples did not show any significant differences in the patterns as it seems similar to each other. The exception of the band present at 1046 cm⁻¹ represents symmetric Si-O-Si meanwhile at 970 cm⁻¹ being a symmetric Si-OH [13]. The absorption bands at 803 cm⁻¹ represent symmetric vibration Si-O [17].

**Figure 5.** FTIR spectra of (a) SiO₂ (b) 1Ni/SiO₂ (c) 3Ni/SiO₂ (d) 5Ni/SiO₂ (e) 10Ni/SiO₂

3.3. Catalytic Testing

The catalytic performance of CO₂ reforming of CH₄ at different nickel loading on SiO₂ was presented in Figure 6(A) and 6(B). While, the effect of Ni loading on the average of CH₄ conversion, CO₂ conversion and product yield of H₂/CO ratio were plotted and presented in Figure 6(C). The catalytic activities of Ni/SiO₂ for CO₂ reforming of CH₄ followed the order of 5Ni/SiO₂ > 3Ni/SiO₂ ≈ 10 Ni/SiO₂ > 1Ni/SiO₂, whereas the average of H₂/CO ratio 5Ni/SiO₂ > 3Ni/SiO₂ > 10Ni/SiO₂ > 1Ni/SiO₂. Poor catalytic activity with less than 5% of CH₄ and CO₂ conversion was observed for unpromoted Ni-SiO₂. This was due to the none available of Ni active site on the surface SiO₂. The most active catalyst was observed for 5Ni/SiO₂ with the conversion of CH₄ and CO₂ of 67.6% and 53.10%, respectively and H₂/CO ratio of 0.91. This achievement was due to the optimum amount of well dispersed Ni active sites which could assist the reaction route. The substitution of sufficient Ni species with the surface silanol groups of SiO₂ was evidenced by FTIR analysis. Moreover, the good dispersion of small Ni particle size in 5Ni/SiO₂ would provide a high surface area, thus enhance catalytic performance. Further increase in Ni loading up to 10wt% was markedly decreased the CH₄ and CO₂ conversion due to the aggregation of Ni species on the surface of SiO₂ as evidenced by XRD. More agglomeration of Ni species would lead to the metal sintering and favor the carbon formation as evidence by TGA analysis. The similar finding was reported by Omoregbe et al. [3], where the higher amount of Ni loading lead to easier sintering and carbon deposition on the surface of SBA-15. The poor catalytic performance of 1Ni/SiO₂ due to the less active site of Ni species and low catalyst stability as evidence by TGA analysis.

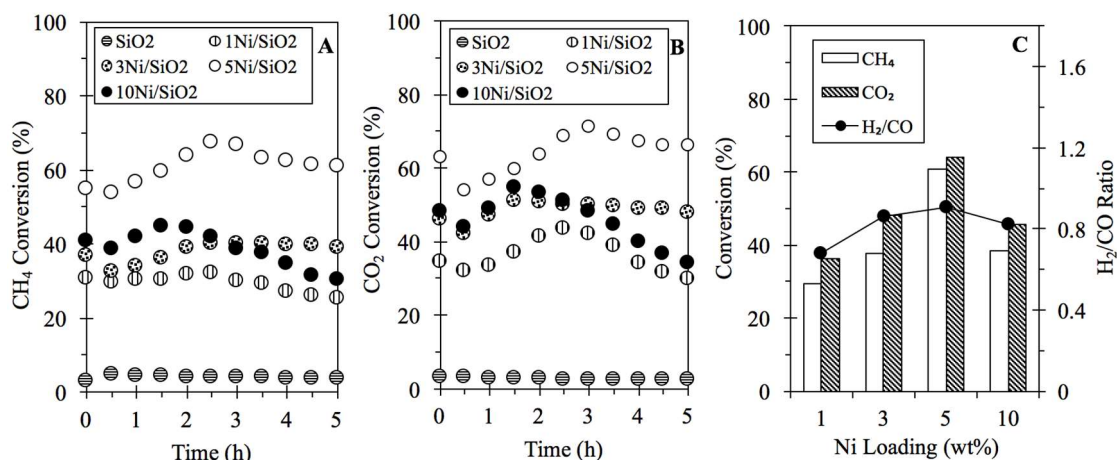


Figure 6. (A) CH₄ conversion and (B) CO₂ conversion of SiO₂, 1Ni/SiO₂, 3Ni/SiO₂, 5Ni/SiO₂, 10Ni/SiO₂ in the CO₂ reforming of CH₄. (C) Effect of Ni loading on the CH₄ conversion, CO₂ conversion, and H₂/CO ratio.

3.4. Characterization of the spent catalysts

Figure 7 shows the TGA analysis for the spent Ni/SiO₂ for the carbon formation after 5 h of time on stream. For all the catalyst, an initial weight loss was observed at 80 °C to 200 °C, which corresponded to the loss water content present in the catalysts. A broad reduction trend was observed at the temperature of 200 °C to 500 °C due to the oxidation of amorphous amorphous silica species [12], while the graphite carbon was oxidized at the temperature more than 500 °C due to the deactivation of Ni/SiO₂ [18]. The amount of carbon content for spent catalyst followed the order 1Ni/SiO₂ (3.13%) < 5Ni/SiO₂ (9.4%) < 3Ni/SiO₂ (10.68%) < 10Ni/SiO₂ (31.36%). It is marked that the weight loss of 5Ni/SiO₂ is very close with the 3Ni/SiO₂ although the Ni loading was different. This result might due to the presence of good interaction of Si-O-Ni in the 5Ni/SiO₂, which inhibited the carbon formation on the surface of the catalyst. Moreover, the less distinction of Ni particle size for both catalysts was also correlated with the carbon formation. The TGA analysis obviously showed that 10Ni/SiO₂ have the highest percentage weight loss due to the burning of carbon deposition in the catalyst. The result displayed that the presence of metal-support interaction can prevent the Ni particle from emerging on the surface of SiO₂ in order to minimize the growth of graphite carbon.

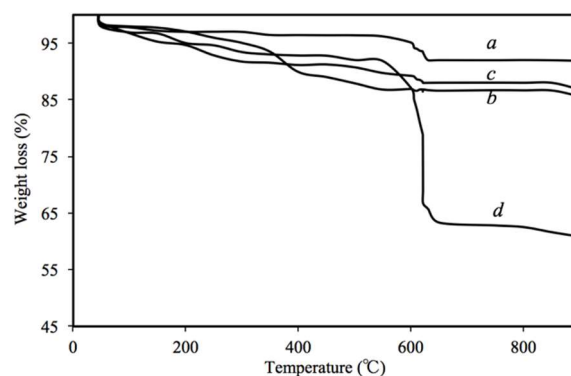


Figure 7. TGA curves of (a) spent 1Ni/SiO₂, (b) 3Ni/SiO₂, (c) spent 5Ni/SiO₂, (d) spent 10Ni/SiO₂, after 5 h reaction

4. Conclusion

In this study, the SiO₂ support was successfully synthesized from Palm Oil Fuel Ash for Ni loading and tested towards CO₂ reforming of CH₄. The influence of Ni loading (1 to 10 wt%) on the support SiO₂

for CO₂ reforming of CH₄ showed the significant influence on the metal support interaction with the performance of the catalytic activity. The characteristics and properties of SiO₂ and Ni/SiO₂ were proven by XRD, BET, FTIR. The catalytic activity of Ni/SiO₂ towards CO₂ reforming of CH₄ followed the order 5Ni/SiO₂ > 3Ni/SiO₂ ≈ 10 Ni/SiO₂ > 1Ni/SiO₂, whereas the average of H₂/CO ratio 5Ni/SiO₂ > 3Ni/SiO₂ > 10Ni/SiO₂ > 1Ni/SiO₂. 5Ni/SiO₂ showed high catalytic activity with CH₄ conversion, CO₂ conversion, and the H₂/CO ratio of 67.6%, 53.10% and 0.91, respectively. The 5Ni/SiO₂ catalyst exhibit superior of catalytic behaviour due to the combination of well dispersion and small size of Ni particle which has potential as a promising catalyst in renewable hydrogen production. In addition, the analysis of spent Ni/SiO₂ proves that the presence of Ni-O-Si minimizes the growth of graphite carbon which enhanced the catalytic stability. The present of metal support interaction, Si-O-Ni played an important role to improve the catalytic performance and prevent coke formation. It can be concluded that POFA waste has good potential to produce SiO₂ as an alternative silica source for the conversion of syngas. In the further study, modification of support needs to be improved in order to produce a better catalytic activity of Ni/SiO₂(POFA).

5. References

- [1] Pan Y-X, Liu C-J and Shi P 2008 Preparation and characterization of coke resistant Ni/SiO₂ catalyst for carbon dioxide reforming of methane *J. Power Sources* **176** 46–53
- [2] Guo J, Lou H, Zhao H, Chai D and Zheng X 2004 Dry reforming of methane over nickel catalysts supported on magnesium aluminate spinels *Appl. Catal. A Gen.* **273** 75–82
- [3] Omoregbe O, Danh H T, Nguyen-Huy C, Setiabudi H D, Abidin S Z, Truong Q D and Vo D V N 2017 Syngas production from methane dry reforming over Ni/SBA-15 catalyst: Effect of operating parameters *Int. J. Hydrogen Energy* **42** 11283–94
- [4] Yao L, Zhu J, Peng X, Tong D and Hu C 2013 Comparative study on the promotion effect of Mn and Zr on the stability of Ni/SiO₂ catalyst for CO₂ reforming of methane *Int. J. Hydrogen Energy* **38** 7268–79
- [5] Koh H, Lee S and Choi J 2004 Conversion of CO₂ to CO with CH₄ over Ni/SiO₂ Catalyst : Photoacoustic Measurements of Reaction Rate *Bull. Korean Chem. Soc.* **25** 1253–6
- [6] Bamaga S O, Hussin M W and Ismail M A 2013 Palm Oil Fuel Ash: Promising supplementary cementing materials *KSCE J. Civ. Eng.* **17** 1708–13
- [7] Lim N H A S, Ismail M A, Lee H S, Hussin M W, Sam A R M and Samadi M 2015 The effects of high volume nano palm oil fuel ash on microstructure properties and hydration temperature of mortar *Constr. Build. Mater.* **93** 29–34
- [8] Budiea A, Hussin M W, Muthusamy K and Ismail M E 2010 Performance of High Strength POFA Concrete in Acidic Environment *Concr. Res. Lett.* **1** 14–8
- [9] Jamo U and Abdu S G 2015 Characterization of a Treated Palm Oil Fuel Ash *Sci. World J.* **10** 27–31
- [10] Irfan Khan M, Azizli K, Sufian S, Man Z and Khan A S 2015 Simultaneous preparation of nano silica and iron oxide from palm oil fuel ash and thermokinetics of template removal *RSC Adv.* **5** 20788–99
- [11] Saharudin K A, Sreekantan S, Basiron N, Chun L K, Kumaravel V, Abdullah T K and Ahmad Z A 2018 Improved super-hydrophobicity of eco-friendly coating from palm oil fuel ash (POFA) waste *Surf. Coatings Technol.* **337** 126–35
- [12] Setiabudi H D, Lim K H, Ainirazali N and Chin S Y 2017 CO₂ reforming of CH₄ over Ni/SBA-15 : Influence of Ni loading on the metal- support interaction and catalytic activity *J. Mater. Environ. Sci.* **8** 573–81
- [13] Lovell E, Scott J and Amal R 2015 Ni-SiO₂ Catalysts for the Carbon Dioxide Reforming of Methane: Varying Support Properties by Flame Spray Pyrolysis *Molecules* **20** 4594–609
- [14] Sidik S M, Triwahyono S, Jalil A A, Aziz M A A, Fatah N A A and Teh L P 2016 Tailoring the properties of electrolyzed Ni/mesostructured silica nanoparticles (MSN) via different Ni-loading methods for CO₂ reforming of CH₄ *J. CO₂ Util.* **13** 71–80

- [15] Zhang P 2016 Adsorption and Desorption Isotherms 10–2
- [16] Ainirazali N, Ainun N, Abghazab N, Setiabudi H D and Yee C S 2017 CO₂ Reforming of Methane over Ni/Ce-SBA-15 : Effects of Ce Addition CO₂ Reforming of Methane over Ni/ Ce-SBA-15 : Effects of Ce Addition **10** 1–5
- [17] Alessi A, Agnello S, Buscarino G and Gelardi F M 2013 Raman and IR investigation of silica nanoparticles structure *J. Non. Cryst. Solids* **362** 20–4
- [18] Majewski A J and Wood J 2014 Tri-reforming of methane over Ni/SiO₂ catalyst *Int. J. Hydrogen Energy* **39** 12578–85

Acknowledgments

The authors gratefully acknowledge the financial support from Universiti Malaysia Pahang through Research Grant Scheme (RDU 170330).